gases

MDPI

Article

Energy and Exergy Analysis of SNG Production from Syngas Derived from Agricultural Residues in Bolívar, Colombia

Ana Buelvas [1,*], Deibys Barreto [2], Hermes Ramírez-León [3] and Juan Fajardo [2]

[1] Department of Mechanical Engineering, Universidad del Norte, Barranquilla 081007, Colombia
[2] Faculty of Engineering, Universidad Tecnológica de Bolívar, Cartagena 130001, Colombia; dbarreto@utb.edu.co (D.B.); jfajardo@utb.edu.co (J.F.)
[3] Mechanical Engineering Program, Universidad Simón Bolívar, Barranquilla 080001, Colombia; hermes.ramirez@unisimon.edu.co
* Correspondence: buelvasana@uninorte.edu.co; Tel.: +57-3104133825

Abstract

Synthetic natural gas (SNG) production from biomass residues represents a promising strategy to reduce greenhouse gas emissions and enhance energy security in regions with abundant agricultural waste. This study evaluates the thermodynamic performance of SNG synthesis from rice husk (RH) and empty fruit bunches (EFB) bio-oils, major residues in the department of Bolívar, Colombia. The process was simulated in Aspen Plus®, integrating syngas data and methanation under equilibrium conditions at 320 °C and 30 bar, complemented by hydrogen injection via alkaline electrolysis to maintain an H_2/CO ratio above 3. Energy and exergy analyses were performed to quantify efficiencies and irreversibilities. Results indicate carbon conversion rates of 48.3% for EFB and 47.4% for RH, producing SNG with 96% CH_4 suitable for grid injection. Energy efficiencies reached 71.9% and 71.0%, while exergy efficiencies were 87.2% and 82.9%, respectively, aligning with or surpassing literature benchmarks. The main irreversibilities occurred in methanation and CO_2 removal, highlighting thermal integration and gas recycling as key improvement strategies. These findings demonstrate the potential of leveraging local biomass for clean energy production and support the development of Power-to-Gas systems in Colombia.

Keywords: synthetic natural gas; biomass gasification; rice husk; empty fruit bunches; aspen plus simulation; energy analysis; exergy analysis; methanation; Power-to-Gas; renewable energy

1. Introduction

Biomass is a promising and environmentally friendly energy source that has the potential to tackle global issues such as climate change, energy scarcity, and ecosystem degradation [1]. However, utilizing biomass efficiently as a renewable energy source remains challenging due to the low combustion efficiency of traditional biomass technologies [2]. Recent advances in biomass gasification, a thermochemical conversion technique, have shown great promise in converting biomass into a high-energy fuel gas, providing a more efficient and potentially sustainable solution [3].

Syngas obtained from the thermochemical conversion of residual biomass constitutes a renewable feedstock with the potential to produce synthetic natural gas (SNG) via methanation [4]. SNG is easily integrated into existing infrastructure and has a lower carbon footprint than other fossil fuels [5]. Therefore, the literature focuses on optimizing

Academic Editor: Călin Baciu

Received: 28 December 2025
Revised: 9 February 2026
Accepted: 13 February 2026
Published: 3 March 2026

synthesis gas generated by steam- and/or oxygen-gasification, characterized by a high H_2/CO ratio and suitable for catalytic processes [6,7].

Methane production via chemical catalysis primarily uses H_2 and CO_2, and H_2 can be obtained through electrolysis or biomass gasification. The latter generates synthesis gas (CO_2 and H_2), from which high-purity H_2 can be separated using gas–liquid or gas–solid systems [8]. Electrolysis, on the other hand, decomposes water into H_2 and O_2 using an electric current, yielding pure H_2 and, when powered by renewable energy, significantly reducing emissions compared to fossil-fuel-based processes.

Furthermore, CO_2 capture from combustion gases has emerged as a leading technology for mitigating atmospheric emissions [8–10]. Additionally, CO_2 produced from biogas, a byproduct of biomass digestion, does not contribute to increased GHG emissions; therefore, its capture and subsequent use or storage could reduce total GHG emissions. Moreover, using this CO_2 as a raw material for various applications adds economic value to a waste stream [11].

On the other hand, syngas can undergo a water–gas conversion reaction, in which CO is converted to CO_2 at approximately 200 °C and 50 bar [12]. This generated CO_2 can also be captured and used as an input in biofuel production processes, such as methane production via methanation reactions [13,14]. The captured CO_2 can be used in the thermochemical conversion process with H_2 to produce methane [15]. Table 1 presents the different technologies for obtaining H_2 and CO_2 for methane synthesis.

Table 1. Sources of H_2 and CO_2 production for methane production.

Author	Source of H_2	Source of CO_2	Process Conditions	Energy Efficiency	Fraction of Methane	LHV SNG
Ciccone et al. [13]	Biomass gasification		350 °C 50 bar	-	26.4 % vol	8.6 MJ/m^3
Michailos et al. [14]	Biomass gasification		-	51.2%	96% vol	-
Szima et al. [8]	Electrolysis Biomass gasification	Captures combustion gases	300 °C 50 bar	57%	94.7% vol	52.4 MJ/m^3
Gorre et al. [9]	Electrolysis	Captures combustion gases	-	78%	-	-
Becker et al. [10]	Electrolysis	Captures combustion gases	-	78%	92.7% vol	47.5 MJ/m^3

Syngas obtained by air gasification exhibits high nitrogen content, which reduces its LHV and makes it unsuitable for injection into the natural gas network or for direct methanation. For this reason, industrial methanation processes typically employ gasification with O_2 or steam, generating a syngas richer in CO and H_2. However, hybrid systems integrating biomass gasification with O_2 and catalytic methanation with renewable H_2 represent a promising alternative, especially in regions with available renewable electricity surpluses. This energy surplus is converted into H_2 through electrolysis and stored as SNG, a more stable and safer energy carrier than pure H_2 during transport and storage [13,16].

Szima et al. [8] investigated the production of SNG from H_2 generated from five different renewable sources: photofermentation, dark fermentation, biomass gasification, biophotolysis, and photovoltaic electrolysis. Of the options evaluated, photofermentation proved to be the most attractive, with a levelized cost of synthetic natural gas of €18.62/GJ in 2020. However, considering production capacities, this option loses its advantages, and biomass gasification becomes more attractive with a slightly higher levelized cost of €20.96/GJ.

Biomass-to-SNG technologies have advanced considerably, particularly in Europe and Asia, where research has focused on optimizing gasification routes, methanation catalysts, and Power-to-Gas integration. However, most reviews and techno-economic assessments emphasize global technological performance and do not examine the applicability of these processes within regions having different biomass profiles and infrastructure constraints. In contrast, the department of Bolívar (Colombia) generates large quantities of agricultural residues that remain underutilized despite their thermochemical potential. According to regional production statistics, Bolívar produces 30,365 t/year of oil-palm residues and 319,388 t/year of rice residues, positioning these feedstocks among the most abundant and stable local biomass streams. Yet, despite this availability, existing studies in Colombia have primarily addressed biomass combustion, biogas, or isolated gasification cases, with no reports evaluating the integrated pyrolysis–gasification-methanation pathway for SNG, nor applying energy and exergy analyses to residues from Bolívar.

This gap is particularly relevant because international air-gasification studies cannot be directly extrapolated to regions like Bolívar, where nitrogen-rich syngas would not meet SNG quality requirements and where renewable electricity intermittency makes hydrogen-assisted methanation an attractive solution. Furthermore, although prior work by Buelvas et al. [17] evaluated the exergy performance of reforming routes for bio-oil, no research has assessed how these syngas streams behave during methanation or how their composition affects carbon conversion, exergy destruction, and SNG quality. Thus, the present study addresses a clear regional and scientific gap by:

1. Evaluating SNG production from the two dominant local residues (EFB and RH).
2. Quantifying energy and exergy performance of their syngas during methanation.
3. Demonstrating the process with Bolívar's biomass and infrastructure.
4. Providing thermodynamic evidence to support local Power-to-Gas development.

This contribution strengthens the study's regional relevance. It also provides a reference for future SNG initiatives in northern Colombia.

Although biomass gasification has traditionally been the main thermochemical route for syngas and methane synthesis, studies that specifically evaluate the integrated biomass pyrolysis—gasification pathway remain limited, particularly regarding detailed energy and exergy assessments. While several reviews and thermo-chemical studies discuss pyrolysis, gasification, or combined stages within broader conversion frameworks, comprehensive evaluations of the pyrolysis—gasification route applied to methane or SNG production are still scarce and virtually absent for contexts such as Bolívar. This study, therefore, contributes by incorporating detailed exergy flows, irreversibilities, and unit efficiencies, providing a deeper understanding of process performance and opportunities for improvement.

Considering that rice husk and empty fruit bunches contribute to the most significant production of residual biomass in the department of Bolívar in Colombia and their cellulose and hemicellulose contents are appropriate to analyze their thermochemical conversion for the production of bio-oil, this study examines the energy and exergy distributions across the methanation stages of synthesis gas produced from the steam reforming of rice husk bio-oil (RH) and empty fruit bunches bio-oil (EFB), following the process developed by Buelvas et al. [17].

2. Materials and Methods

2.1. Syngas Composition

According to the Mining and Energy Planning Unit, in 2019, in the region of Bolívar, Colombia, the generation of waste from oil palm cultivation amounted to 30,365 tons annually, of which 21–23% corresponded to empty fruit bunches [18,19]. On the other

hand, rice production generated approximately 319,388 tons of waste annually, of which an estimated 20% corresponded to rice husks [20–22].

Therefore, in this study, 697 kg/h of EFB and RH waste were used to produce bio-oil using the pyrolysis simulation developed by Buelvas et al. [17]. Table 2 shows the molar fractions and mass flow rates of the syngas obtained from the steam reforming of bio-oil derived from oil palm empty fruit bunches (EFB) and rice husk (RH) at a steam–bio-oil ratio of 0.25 at 800 °C.

Table 2. Molar fraction and mass flow rates of the syngas obtained from the gasification of bio-oil [17].

Syngas Component	Bio-Oil Type	
	EFB	RH
H_2O	0.15	0.23
H_2	0.49	0.43
CO_2	0.09	0.06
CO	0.27	0.28

These syngas streams, with flow rates of 432 kg/h for EFB bio-oil and 370 kg/h for RH bio-oil, will serve as feedstock for the subsequent methanation process. The main components considered are H_2O, H_2, CO_2, and CO, with their respective molar fractions indicated for each case.

The agricultural residues available in the department of Bolívar, particularly rice husk (RH) and empty fruit bunches (EFB), exhibit physicochemical characteristics that significantly influence their thermochemical conversion behavior, thereby distinguishing this study from previous biomass-to-SNG research. Both RH and EFB exhibit high cellulose and hemicellulose contents, which promote greater devolatilization and bio-oil production during fast pyrolysis, enabling the subsequent steam reforming stage used to generate syngas in this work. High holocellulose fractions favor the release of H_2 and CO precursors at 700–800 °C, which directly affects the H_2/CO ratio obtained during reforming and, consequently, the performance of the methanation step.

Rice husk additionally contains one of the highest ash fractions within agricultural residues, with a substantial proportion of silica. This high inorganic content affects heat transfer, catalytic activity of inherent minerals, and tar cracking behavior during pyrolysis and steam reforming, producing a syngas with a distinct composition compared to woody biomass typically used in SNG studies. EFB, in contrast, has a lower ash content but a higher volatile fraction and higher hemicellulose content, which increase reactivity and enhance hydrogen release during reforming. These compositional differences explain the slightly higher H_2 content in EFB-derived syngas (0.49) compared to RH (0.43) and the higher water fraction in RH syngas (0.23), as reported in Table 2. Both factors strongly influence the equilibrium of the methanation reactions evaluated in this work.

These physicochemical attributes are seldom analyzed in previous SNG studies, which typically consider generic lignocellulosic biomass or wood-based feedstocks with more homogeneous compositions. This study explicitly evaluates SNG production from two tropical residues. It characterizes how their holocellulose content and ash composition impact syngas quality, carbon conversion, exergy destruction, and overall methanation performance.

2.2. Process Description

For SNG synthesis, an H_2/CO ratio greater than three must be maintained [23]. Furthermore, studies indicate that, in electrolysis and integrated gasification processes, SNG synthesis is favored at 250–320 °C and 20–50 bar [8,24,25]. Moreover, kinetic barriers are minimized, and the mixture reaches equilibrium, making a kinetic reactor block such as

RPlug unnecessary [26,27]. The process developed in Aspen Plus® to obtain the flow rates required for methanation is described below.

The process model is implemented using the RGibbs block at 320 °C and 30 bar, which calculates the overall chemical equilibrium by minimizing the Gibbs free energy. The Sabatier reactions, the water–gas shift (WGS) reaction, and the methanation of CO take place in this block, represented in Equations (1)–(3), respectively [8,14].

$$CO_2 + 4H_2 \rightarrow CH_4 + 2H_2O \quad -165 \frac{\text{kJ}}{\text{kmol}} \tag{1}$$

$$CO + H_2O \rightarrow H_2 + CO_2 \quad -41.2 \frac{\text{kJ}}{\text{kmol}} \tag{2}$$

$$CO + 3H_2 \rightarrow CH_4 + H_2O \quad -206.2 \frac{\text{kJ}}{\text{kmol}} \tag{3}$$

The process diagram for SNG production is shown in Figure 1. The process consists of four main stages: synthesis gas compression, electrolysis, SNG synthesis, and phase separation.

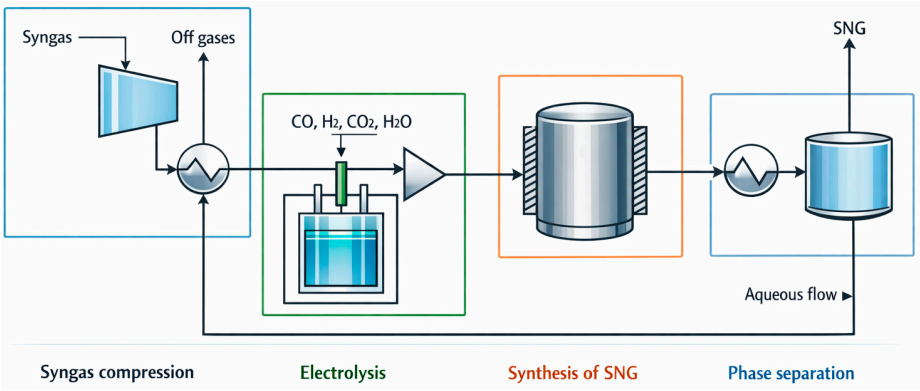

Figure 1. Schematic diagram of the SNG production process.

In the compression stage, a COMP block with an isentropic efficiency of 0.85 and a heat block are used to lower the gas temperature so that the synthesis gas enters the synthesis stage at 320 °C and 30 bar. During the synthesis stage in the RGibbs block, chemical equilibrium is established at the specified pressure and temperature. In the phase section, the option to include the vapor phase is enabled, and the maximum number of solid phases is set to 0 to restrict the calculation to species present in the gas phase. This resulted in the equilibrium distribution of the species CH_4, CO_2, H_2, and H_2O. Then, in the separation stage, a flash block at 25 °C and 50 bar is used to separate the stream from the RGibbs block into its liquid and gaseous phases. The residual aqueous flow is recirculated to the heat exchanger to harness the energy of the cold fluid, cooling the high-temperature syngas stream down to 320 °C.

On the other hand, the electrolysis simulation model was developed for an alkaline electrolyzer. Specifically, it is modeled in an RStoic reactor to produce H_2, ensuring the H_2/CO ratio required for SNG synthesis. In this study, an H_2/CO ratio greater than three is guaranteed. Two flow streams were used to produce H_2: the first flow stream contains H_2O and KOH with mass fractions of 0.2 and 0.8, respectively, while the second flow stream entering the electrolyzer contains only H_2O.

In the alkaline electrolysis model, the RStoic reactor provides a simplified stoichiometric representation. However, it is important to acknowledge the influence of operating parameters on electrolysis performance. In practical systems, both temperature and electrolyte concentration directly affect cell voltage and ionic conductivity. Higher

temperatures reduce ohmic losses. Appropriate KOH concentrations (20 wt%) enhance conductivity without causing viscosity issues. The electrolyte composition used in this study (H_2O/KOH = 0.2/0.8) reflects typical alkaline operation conditions. Although Aspen estimates power consumption through a design-specification block, assuming an overall electrolyzer efficiency, variations in these parameters would proportionally affect electrical demand and, consequently, the global energy and exergy efficiencies. This clarification strengthens the physical basis of the electrolysis module within the system-level evaluation.

Finally, a design specification block is used to estimate the electrical consumption of the RStoic block to achieve the required H_2 molar flow rate in each study scenario. The results of this electrolysis model are validated through the calculation of the electrolyzer efficiency $(n_{electrolyzer})$ denoted in Equation (4). Where $\dot{m}_{H_2}$, LHV_{H_2} y $\dot{W}_{electrolyzer}$ represent the mass flow of H_2, the lower heating value of H_2, and the electrical energy consumed by the electrolyzer, respectively.

$$n_{electrolyzer} = \frac{\dot{m}_{H_2} \times LHV_{H_2}}{\dot{W}_{electrolyzer}} \quad (4)$$

The methanation stage was modeled using the RGibbs reactor, which calculates the equilibrium composition by minimizing the system's Gibbs free energy at fixed temperature and pressure. Since the selected operating conditions (320 °C and 30 bar) fall within the range where methanation reactions approach equilibrium, the RGibbs formulation is aligned with the thermodynamic behavior expected for high H_2/CO ratios. To ensure the reliability of the model results, a validation procedure was carried out by comparing them with published experimental and pilot-scale methanation data.

First, the model predicts an equilibrium CH_4 content of 96% in both scenarios, which matches the methane fractions reported (94–97%) in high-pressure methanation experiments and Aspen-based equilibrium studies under similar conditions (300–350 °C, 20–50 bar). This agreement confirms that the model reproduces expected thermodynamic limits. Furthermore, the CO and CO_2 conversions align with previously reported methane yields for equilibrium methanation at H_2/CO ratios above 3, further supporting the accuracy of equilibrium-based predictions under these conditions.

Second, the energy and exergy efficiencies calculated by the model (71–71.9% for energy and 82.9–87.2% for exergy) are within or above the ranges reported in Aspen Plus equilibrium simulations. This reinforces that the applied thermodynamic framework provides results consistent with published equilibrium simulation data.

Finally, it should be noted that the RGibbs equilibrium model assumes idealized reactor behavior, free of kinetic or transport limitations. However, because the methanation reactions are highly exothermic and approach equilibrium at moderate temperatures under H_2-rich conditions, especially when the H_2/CO ratio exceeds 3, the equilibrium approach is widely used for preliminary design, optimization, and thermodynamic assessments. The agreement between the equilibrium predictions and previously reported pilot-scale data supports the adequacy of the modeling strategy adopted in this study.

2.3. Energy and Exergy Analysis

Aspen Plus enabled estimation of the energy requirements for SNG synthesis. Furthermore, the physical exergy of the stream was obtained from the Aspen Plus results. However, additional equations were required to estimate the chemical exergy. Figure 2 shows the streams considered in the energy and exergy estimates of the SNG synthesis process.

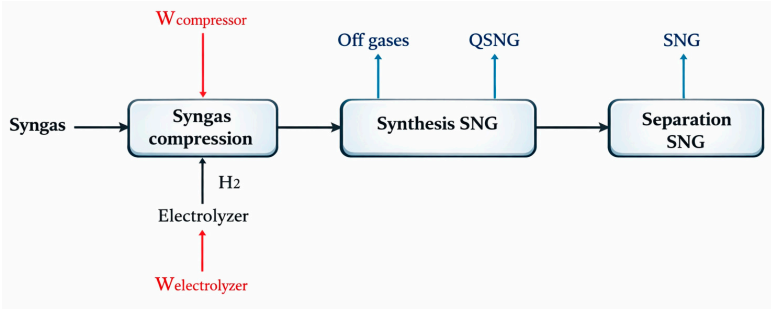

$$Q_{out} = Q_{SNG}$$

$$W_{in} = W_{compressor} + W_{electrolyzer}$$

Figure 2. Schematic diagram summarizing the main streams used for the energy and exergy calculations of the SNG synthesis stage applied in each scenario.

Equations (5)–(10) show the energy and exergy balances. In these equations, $\dot{m}$ indicates the mass flow rate, where the subscripts in and out represent the input and output, respectively. Equations (6) and (7) are the steady-state energy and exergy balances, respectively, where $\dot{E}$ represents the energy flow rate and $\dot{X}$ the total exergy (Equation (8)). The exergy includes physical ($\dot{X}_{ph}$) and chemical ($\dot{X}_{ch}$), components, estimated using Equations (9) and (10), respectively.

$$\sum \dot{m}_{in} = \sum \dot{m}_{out} \tag{5}$$

$$\sum \dot{E}_{in} = \sum \dot{E}_{out} \tag{6}$$

$$\sum \dot{X}_{in} = \sum \dot{X}_{out} + \sum \dot{X}_{dest} \tag{7}$$

$$\dot{X} = \dot{X}_{ph} + \dot{X}_{ch} \tag{8}$$

$$\dot{X}_{ph} = \dot{m}[h - h_0 - T_0(s - s_0)] \tag{9}$$

$$\dot{X}_{ch} = \dot{n}\sum x_i \left(x_i^{ch} + RT_0 ln x_i\right) \tag{10}$$

The terms h y s represent the specific enthalpy and entropy, respectively, while h_0, T_0, y s_0 denote the dead-state enthalpy, temperature, and entropy (298.15 K and 101.325 kPa). Similarly, x_i indicates the mole fraction of component i, $\dot{n}$ is the molar flow rate, R corresponds to the universal gas constant, and x_i^{ch} is the standard chemical exergy of component i.

The equations used to calculate energy and exergy efficiency in the SNG synthesis process are described below.

Equation (11) allowed the calculation of the energy efficiency η_t^{SNG} in the SNG synthesis stage. Here, $\dot{E}_{SNG}$ is the energy achieved by the SNG stream, while $\dot{E}_{in}^{SNG}$ represents the energy from the synthesis gas and the input power.

$$\eta_t^{SNG} = \frac{\dot{E}_{SNG}}{\dot{E}_{in}^{SNG}} \tag{11}$$

Equation (12) was used to calculate the exergy efficiency η_{Ex}^{SNG} of the SNG synthesis process. Where $\dot{X}_{\mathrm{SNG}}$ is the exergy harnessed by the methane stream in the distillation stage of the process according to the evaluated scenario, while $\dot{X}_{in}^{\mathrm{SNG}}$ represents the exergy from the synthesis gas, the heat input, and the power supplied.

$$\eta_{Ex}^{SNG} = \frac{\dot{X}_{SNG}}{\dot{X}_{in}^{SNG}} \quad (12)$$

3. Results

3.1. Carbon Conversion

Carbon conversion is a key indicator of methanation process efficiency, as it reflects the percentage of carbon in syngas that is converted to methane (CH_4). This parameter allows us to determine the degree of resource utilization and the technical viability of the process under different conditions and with other raw materials. This study analyzes two scenarios: the first corresponds to syngas obtained by gasification of bio-oil from EFB (experimental biofuels). At the same time, the second is based on bio-oil from RH (renewable hydrocarbons). Comparing these two scenarios allows us to identify the impact of biomass type on conversion efficiency and to identify opportunities to improve synthetic natural gas (SNG) production.

The results obtained in Table 3 show that the carbon conversion in the methanation of syngas derived from EFB (48.3%) and RH (47.4%) bio-oils is similar, demonstrating the technical viability of the process for different residual feedstocks. This closeness in values indicates that the type of biomass does not significantly affect efficiency under the evaluated conditions, thus conferring robustness to the system. The observed efficiency is explained by the exothermic nature of the methanation reaction, which favors CH_4 formation at moderate temperatures, thereby reducing carbon losses.

Table 3. Carbon conversion to syngas methanation for scenarios evaluated.

Scenario	Carbon Conversion (%)
Scenario 1	48.3
Scenario 2	47.4

Although the conversion is within the typical range for pilot processes, with almost half of the carbon transformed into CH_4, there is significant room for optimization. Factors such as the H_2/CO ratio, operating pressure, recycling of unconverted gases, and the selection of more active catalysts could increase the conversion to industrial levels (>80%). These results are relevant because they demonstrate the potential of utilizing Colombian agricultural waste to produce synthetic natural gas, contributing to energy sustainability and emissions reduction.

3.2. Energy and Exergy Analysis Results

This section analyzes the energy and exergy distribution of SNG synthesis. The volumetric composition of CH_4 and CO_2 in the SNG is 96% and 4%, respectively, in both scenarios. Figure 3 shows the Sankey diagrams of the energy distribution of the SNG synthesis process for Scenarios 1 and 2. In Scenario 1, the process's energy efficiency is 71.9%, while in Scenario 2 it reaches 71%. The energy efficiency of the methanation process is slightly higher (0.9%).

This implies that a larger fraction of the carbon is in the form of CO_2, which reduces simultaneous chemical reactions and decreases the thermal load on the reactor. These conditions reduce irreversibilities and allow for slightly better utilization of the available energy during methanation.

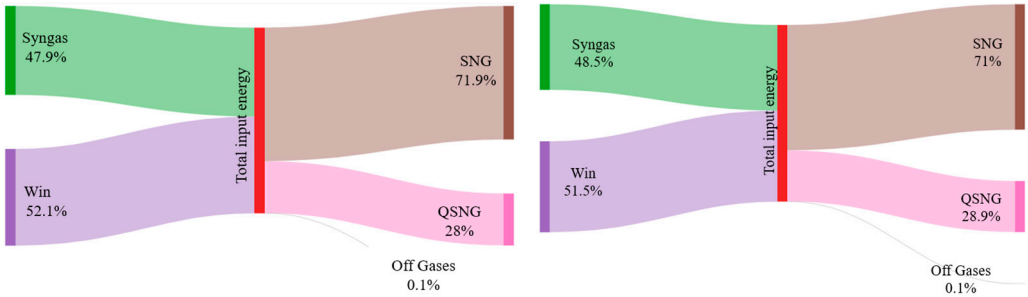

(**a**) Scenario 1 (**b**) Scenario 2

Figure 3. Sankey diagrams of the energy distribution for SNG synthesis, (**a**) Scenario 1 and (**b**) Scenario 2.

Given the weight of electricity in the balance (51–52%), thermal integration to recover QSNG and optimize electrolysis and compression is emerging as the main lever to raise the effective efficiency of the process, with the potential to exceed 80% when the available heat is partially recovered.

Moreover, Figure 4 presents the Sankey diagram of the exergy distribution for the SNG synthesis stage, evaluated in Scenarios 1 and 2. In Scenario 1, the process exergy efficiency is 87.2%, while in Scenario 2 it is 82.9%. This 4.3% difference is due to lower exergy destruction during the methanation stage in Scenario 1. In this scenario, the addition of H_2 optimizes the H_2/CO ratio, improves the conversion of synthesis gas, and recovers chemical energy into useful exergy in SNG, reducing heat losses and irreversibilities.

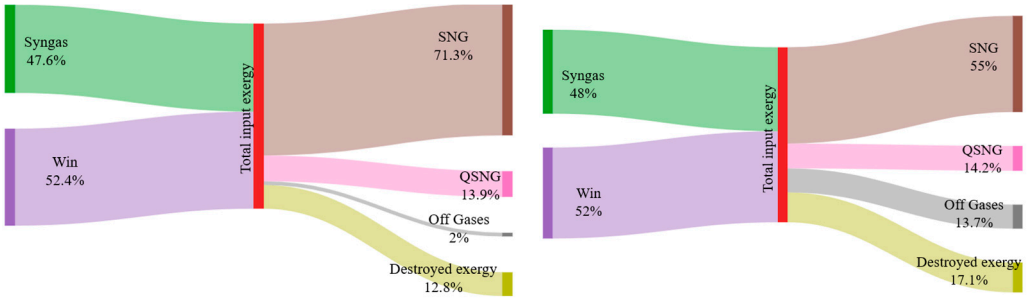

(**a**) Scenario 1 (**b**) Scenario 2

Figure 4. Sankey diagrams of the exergy distribution for SNG synthesis, (**a**) Scenario 1 and (**b**) Scenario 2.

Furthermore, Scenario 1 exhibits almost negligible off-gas losses (2%) and lower exergy destruction (12.8%), while in Scenario 2, blowdown accounts for a significant fraction of exergy (13.7%) and internal irreversibilities are higher (17.1%), indicating operation further from the thermodynamic optimum. The QSNG confirms the exothermic nature of the system and represents the main opportunity for thermal recovery. In summary, Scenario 1 better utilizes the available work potential and operates with lower irreversibilities. In contrast, Scenario 2 requires reduced blowdown, thermal integration, and fine-tuning of the H_2/CO catalytic activity ratio to decrease exergy destruction and improve its second-law performance.

Table 4 presents the energy and exergy efficiencies of the process evaluated in the two study scenarios. The differences in energy efficiency among the studied scenarios were influenced by the type of raw material and its composition, the operating conditions, the bio-oil composition, and steam consumption. The results of this study are consistent with those reported in the literature for SNG synthesis processes developed in Aspen Plus®. These thermochemical processes achieve energy efficiencies exceeding 70% and exergy efficiencies between 70 and 87%, especially when incorporating heat recovery and

an H_2/CO ratio of 3 [10,28–30]. Table 4 summarizes the research evaluating their energy and exergy performance.

Table 4. Comparison of the energy and exergy efficiency of SNG synthesis in the different scenarios.

Author	CO_2	H_2	Block Aspen	Temperature °C	Pressure Bar	η_t (%)	η_{Ex} (%)
Juraščík et al. [29]	Syngas		RGIBBS	405–580	1–30	-	69.5–71.8
Kesha et al. [28]	Capture Natural Gas	Electrolysis	RGIBBS	313	1	74.3–76.4	84–87%
Becker et al. [10]	Syngas	Electrolysis	RPLUG	300–350	30	81.2	-
Zakwani et al. [31]	Syngas	Electrolysis Syngas	RPLUG	250–400	27	44–59	-
Duret et al. [30]	Electrolysis		RPLUG	350–550	20–30	-	72.6
Scenario 1	Syngas	Electrolysis	RPLUG	320	30	71.9	87.2
Scenario 2	Syngas	Electrolysis	RPLUG	320	30	71	82.9

The results of Juraščík et al. [29] show that the main irreversibilities are concentrated in the gasifier, the methanation section, and the CO_2 capture unit. At the same time, the gas compression and cleaning stages exhibit minor losses. The overall exergy efficiency of the process ranged from 69.5% to 71.8%, with a maximum of 71.8% at 650 °C and 15 bar, conditions that favor higher SNG production and reduce the need for cooling in the methanation reactors. The SNG obtained had a CH_4 composition of 79.8–86 mol%, an HHV of 33–35 MJ/Nm^3, and a Wobbe index of 44 MJ/Nm^3, meeting the quality standards for grid injection. Overall, the work demonstrates that thermodynamic optimization of the biomass-SNG process can achieve efficiencies higher than those reported for other biofuels.

Kesha et al. [28] developed a thermo-exergy model of a Power-to-Gas (PtG) process coupled with high-temperature electrolysis (HTCE) to convert CO_2 and water vapor into SNG, using Aspen Plus (V8.4) simulations. The results show that the electrolyzer is responsible for the most incredible exergy destruction, due to the high energy demand of the electrolysis process. At the same time, the methanation and compression stages exhibit lower exergy losses. However, the final composition of the product gas (21.4% CH_4, 76.5% CO_2) does not meet the standards for grid injection, concluding that HTCE is unsuitable for producing SNG, but viable as a route for generating syngas intended for the synthesis of liquid fuels with a higher C/H ratio.

Biological or hybrid systems, such as the one proposed by Michailos et al. [14], exhibit overall efficiencies close to 50%, a lower value than that of thermochemical processes due to the inherent kinetic limitations of fermentation and the lower conversion of synthesis gas. In contrast, more recent studies, such as those by Becker et al. [10] and Al Zakwani et al. [31], demonstrate that H2 injection is the most effective strategy for increasing energy efficiency and reducing exergy destruction, as it promotes a more complete conversion of CO and CO_2 to CH_4 under controlled conditions. Furthermore, most of these processes operate at 300–400 °C and 20–30 bar, parameters consistent with Scenarios 1 and 2 simulated in Aspen Plus® in this study, confirming the thermodynamic and operational validity of the selected conditions. Finally, to make SNG more attractive and competitive, improving the plant's overall exergetic efficiency is an important issue [29].

4. Discussion

The results confirm that the production of SNG from agricultural waste, namely rice husk (RH) and empty palm bunches (EFB), is technically viable and relevant for the department of Bolívar. These local streams, currently underutilized, can reliably feed the

thermochemical route: (1) pyrolysis, (2) steam reforming, followed by (3) methanation, evaluated in this work, creating a value chain for the palm and rice sectors and contributing to the energy security of the territory [30].

The small differences observed between EFB and RH can be explained by the intrinsic properties of each biomass. EFB typically contains more volatiles and a higher hemicellulose fraction. This enhances reactivity during pyrolysis and steam reforming, resulting in slightly higher H_2 content in the resulting syngas (0.49 vs. 0.43 for RH). In contrast, RH has a significantly higher ash content, which is dominated by silica. This reduces the effective organic fraction available for conversion and increases the proportion of inert material. As a result, RH syngas shows a higher water fraction (0.23) and slightly lower carbon conversion (47.4% vs. 48.3% for EFB). Additionally, ash in RH can limit heat transfer during reforming and increase exergy destruction, which aligns with the lower exergetic efficiency in Scenario 2. These feedstock-dependent differences clarify the mechanism behind the reported trends and reinforce the importance of evaluating region-specific biomass when assessing SNG production performance.

The resulting SNG exhibits grid-quality (96% CH_4 and 4% CO_2) in both scenarios, with energy efficiencies of 71.9% (EFB) and 71.0% (RH), and exergy efficiencies of 87.2% and 82.9%, respectively. These values are within and even above the typical exergy ranges reported for simulated processes in Aspen, where the overall exergy efficiency of the biomass train to SNG is usually between 69.5 and 71.8% and can scale up to 72.6% under optimal operating conditions [30]. In this work, the heat transfer of the system and the weight of electricity (51–52% of the balance) indicate that thermal integration (heat recovery for compression and electrolysis) is the main lever to raise the effective efficiency above 80%, consistent with design recommendations and energy-economic integration in the literature.

Carbon to CH_4 conversion reached 48.3% (EFB) and 47.4% (RH), with minimal off-gas losses in Scenario 1 and greater purge in Scenario 2. Although these values are consistent with pilot scales, the literature shows that adjustments in H_2/CO, pressure, and cooling strategy allow conversion to be increased to 50–60% at the whole train level and exceed 80% in industrial operation with recycles and more active catalysts, reinforcing that there is room for optimization on an already thermally and exergetically sound basis [27].

The findings of this study replicate the thermo-exergetic patterns observed by Juraščík et al. [27], where the greatest irreversibilities are concentrated in the gasifier, the methanation section, and the CO_2 capture. Furthermore, lower methanation temperatures and higher gasification pressures increase overall exergetic efficiency, and the selection of adiabatic or intermediate-cooled reactor operation should be based on the methane already produced in the gasifier and the risk of catalyst overheating. The energy and exergetic Sankey diagrams in this work reproduce this loss distribution and the beneficial effect of improving the H_2/CO ratio before methanation, consistent with these references.

Furthermore, Duret et al. [30] demonstrate that, even with thermal efficiencies of 58%, thermal integration can supply most of the mechanical work of compression, substantially reducing the net electrical demand of the process. The heat in methanation aligns with this practical possibility in the Bolívar case, where the available heat could be recovered for preheating, process steam generation, and compressor/electrolyzer support.

Regarding operational and design implications, simulation with alkaline electrolysis to adjust H_2 while maintaining 320 °C and 30 bar in the RGibbs block minimizes kinetic barriers and improves Sabatier and WGS equilibrium, consistent with reference thermochemical pathways. The selection of Ni with WGS activity and steam addition is consistent with reported practices to avoid carbon formation and control thermal spikes; it is suggested that promoted Ni or supports with improved heat transfer be evaluated for stable operation in the 250–320 °C/20–50 bar range [27].

With SNG compositions of 96% CH_4 suitable for injection and efficiencies in line with the best available evidence, the system can decarbonize industrial thermal uses (rice mills, palm oil extraction plants) by replacing fossil gas; it can also valorize waste and reduce CH_4 emissions from traditional disposal; as well as enable a local Power-to-Gas scheme when there is a surplus of renewable electricity to produce H_2 by electrolysis and store it as SNG, which is safer and more stable than pure H_2 in transport; and strengthen a circular economy with rural employment and additional income for the rice and palm oil value chains.

This study is based on chemical equilibrium (Gibbs free energy) for methanation and a stoichiometric model for electrolysis. Although adequate for exploring thermo-exergetic performance, future validation should include kinetics and heat transfer of a specific catalyst; detailed thermal integration (heat exchanger network) for heat recovery as high-pressure steam; optimization of purge/recycling and CO_2 capture; and comparison with experimental data from gasification/pyro-reforming of bio-oil from RH and EFB at pilot scale. These actions are aligned with the recommendations for improving exergetic efficiency and thermal management reported by Juraščík et al. [27] and Duret et al. [30].

This work demonstrates technical validity and scientific coherence: it delivers high-quality SNG, efficiencies comparable to or exceeding benchmarks, and a thermal integration strategy that can translate into electricity savings and greater operational robustness. Given the potential for waste from hydroelectric and biofuel production in Bolívar, the territorial impact is clear: clean energy, local added value, and emissions reduction.

5. Conclusions

The study demonstrates that producing natural gas from agricultural waste in the department of Bolívar—rice husks and empty palm bunches—is technically feasible and aligns with local biomass availability. This approach contributes to the valorization of agro-industrial byproducts, reduces emissions associated with their traditional disposal, and strengthens regional energy security.

Simulations in Aspen Plus® yielded energy efficiencies exceeding 70% and exergy efficiencies between 82.9% and 87.2%, values comparable to or exceeding those reported in the literature for biomass-to-SNG processes (69.5–72.6%). These results confirm the thermodynamic robustness of the proposed scheme and its potential for optimization through thermal integration.

Carbon conversion reached approximately 48%, generating a gas with 96% CH_4, suitable for injection into natural gas networks. Although these values are typical of pilot-scale operations, the literature indicates that adjusting the H_2/CO ratio, pressure, and gas recycling can raise conversion to industrial levels (>80%).

The main lever for increasing overall efficiency is recovering methanation heat and using it for compression and electrolysis, enabling energy efficiency exceeding 80%. Likewise, optimizing purge, integrating heat exchangers, and selecting more active catalysts are recommended strategies to reduce irreversibilities and improve second-law performance.

This work lays the groundwork for a Power-to-Gas scheme in Bolívar, capable of storing surplus renewable electricity as SNG, a safer and more stable energy vector than pure H_2. Furthermore, it promotes a circular economy that generates added value, creates rural employment, and reduces emissions, aligning with energy sustainability and decarbonization goals.

Author Contributions: Conceptualization, A.B.; methodology, A.B. and J.F.; software, A.B.; validation, A.B., J.F. and D.B.; formal analysis, A.B. and J.F.; investigation, A.B.; data curation, A.B.; writing—original draft preparation, A.B.; writing—review and editing, D.B.; writing—review and editing,

H.R.-L. and J.F.; visualization, A.B.; project administration, A.B. All authors have read and agreed to the published version of the manuscript.

Funding: This research was supported by MINCIENCIAS through the "Beca Nacional de Doctorado—Becas Bicentenario 2019", under Contract UN-OJ-2020-47412.

Data Availability Statement: The original contributions presented in this study are included in the article. Further inquiries can be directed to the corresponding author(s).

Acknowledgments: The authors gratefully acknowledge the support provided by MINCIENCIAS for the doctoral scholarship support.

Conflicts of Interest: The authors declare no conflicts of interest.

Abbreviations

The following abbreviations are used in this manuscript:

SNG	Synthetic Natural Gas
RH	Rice Husk
EFB	Empty Fruit Bunches
WGS	Water–Gas Shift
LHV	Lower Heating Value
PtG	Power-to-Gas

References

1. Gao, Y.; Wang, M.; Raheem, A.; Wang, F.; Wei, J.; Xu, D.; Song, X.; Bao, W.; Huang, A.; Zhang, S.; et al. Syngas Production from Biomass Gasification: Influences of Feedstock Properties, Reactor Type, and Reaction Parameters. *ACS Omega* **2023**, *8*, 31620–31631. [CrossRef]
2. Doherty, W.; Reynolds, A.; Kennedy, D. Aspen plus simulation of biomass gasification in a steam blown dual fluidised bed. In *Materials and Processes for Energy*; Formatex Research Centre: Norristown, PA, USA, 2013; pp. 212–220.
3. Sikarwar, V.S.; Zhao, M.; Clough, P.; Yao, J.; Zhong, X.; Memon, M.Z.; Shah, N.; Anthony, E.J.; Fennell, P.S. An overview of advances in biomass gasification. *Energy Environ. Sci.* **2016**, *9*, 2939–2977. [CrossRef]
4. Kumar, R.N.; Aarthi, V. From biomass to syngas, fuels and chemicals—A review. In *AIP Conference Proceedings*; American Institute of Physics Inc.: College Park, MD, USA, 2020. [CrossRef]
5. Mäki-Arvela, P.; Aho, A.; Simakova, I.; Yu, D. *Murzin, Sustainable Aviation Fuel from Syngas Through Higher Alcohols*; John Wiley and Sons Inc.: Hoboken, NJ, USA, 2022. [CrossRef]
6. Koytsoumpa, E.I.; Karellas, S. Equilibrium and kinetic aspects for catalytic methanation focusing on CO_2 derived Substitute Natural Gas (SNG). *Renew. Sustain. Energy Rev.* **2018**, *94*, 536–550. [CrossRef]
7. Song, G.; Xiao, J.; Yan, C.; Gu, H.; Zhao, H. *Quality of Gaseous Biofuels: Statistical Assessment and Guidance on Production Technologies*; Elsevier Ltd.: Amsterdam, The Netherlands, 2022. [CrossRef]
8. Szima, S.; Cormos, C.C. CO_2 utilization technologies: A techno-economic analysis for synthetic natural gas production. *Energies* **2021**, *14*, 1258. [CrossRef]
9. Gorre, J.; Ortloff, F.; van Leeuwen, C. Production costs for synthetic methane in 2030 and 2050 of an optimized Power-to-Gas plant with intermediate hydrogen storage. *Appl. Energy* **2019**, *253*, 113594. [CrossRef]
10. Becker, W.L.; Penev, M.; Braun, R.J. Production of synthetic natural gas from carbon dioxide and renewably generated hydrogen: A techno-economic analysis of a power-to-gas strategy. *J. Energy Resour. Technol. Trans. ASME* **2019**, *141*, 021901. [CrossRef]
11. Cordova, S.S.; Gustafsson, M.; Eklund, M.; Svensson, N. Potential for the valorization of carbon dioxide from biogas production in Sweden. *J. Clean. Prod.* **2022**, *370*, 133498. [CrossRef]
12. Rao, S.; Han, Y.; Ho, W.S.W. *Recent Advances in Polymeric Membranes for Carbon Dioxide Capture from Syngas*; Taylor and Francis Ltd.: Oxfordshire, UK, 2023. [CrossRef]
13. Ciccone, B.; Murena, F.; Ruoppolo, G.; Urciuolo, M.; Brachi, P. Methanation of syngas from biomass gasification: Small-scale plant design in Aspen Plus. *Appl. Therm. Eng.* **2024**, *246*, 122901. [CrossRef]
14. Michailos, S.; Emenike, O.; Ingham, D.; Hughes, K.J.; Pourkashanian, M. Methane production via syngas fermentation within the bio-CCS concept: A techno-economic assessment. *Biochem. Eng. J.* **2019**, *150*, 107290. [CrossRef]
15. de Kleijne, K.; Hanssen, S.V.; van Dinteren, L.; Huijbregts, M.A.J.; van Zelm, R.; de Coninck, H. Limits to Paris compatibility of CO_2 capture and utilization. *One Earth* **2022**, *5*, 168–185. [CrossRef]

16. Kiendl, I.; Klemm, M.; Clemens, A.; Herrman, A. Dilute gas methanation of synthesis gas from biomass gasification. *Fuel* **2014**, *123*, 211–217. [CrossRef]
17. Buelvas, A.; Quintero-Coronel, D.A.; Vanegas, O.; Ortegon, K.; Bula, A.; Mesa, J.; González-Quiroga, A. Gasification of solid biomass or fast pyrolysis bio-oil: Comparative energy and exergy analyses using AspenPlus®. *Eng. Rep.* **2024**, *6*, e12825. [CrossRef]
18. Awoh, E.T.; Kiplagat, J.; Kimutai, S.K.; Mecha, A.C. *Current Trends in Palm Oil Waste Management: A Comparative Review of Cameroon and Malaysia*; Elsevier Ltd.: Amsterdam, The Netherlands, 2023. [CrossRef]
19. Liew, W.L.; Kassim, M.A.; Muda, K.; Loh, S.K. Feasibility Study on Palm Oil Processing Wastes Towards Achieving Zero Discharge Malaysian Palm Oil Board. 2016. Available online: https://www.researchgate.net/publication/303370504 (accessed on 17 December 2025).
20. Yuan, S.; Hou, Y.; Liu, S.; Ma, Y. A Comparative Study on Rice Husk, as Agricultural Waste, in the Production of Silica Nanoparticles via Different Methods. *Materials* **2024**, *17*, 1271. [CrossRef] [PubMed]
21. Bodie, A.R.; Micciche, A.C.; Atungulu, G.G.; Rothrock, M.J.; Ricke, S.C. Current Trends of Rice Milling Byproducts for Agricultural Applications and Alternative Food Production Systems. *Front. Sustain. Food Syst.* **2019**, *3*, 47. [CrossRef]
22. Ramírez, A.T.O.; Tovar, M.R.; Silva-Marrufo, O. Rice husk reuse as a sustainable energy alternative in Tolima, Colombia. *Sci. Rep.* **2024**, *14*, 10391. [CrossRef] [PubMed]
23. He, Z.; Wang, X.; Gao, S.; Xiao, T. Effect of reaction variables on CO methanation process over NiO–La_2O_3–MgO/Al_2O_3 catalyst for coal to synthetic natural gas. *Appl. Petrochem. Res.* **2015**, *5*, 413–417. [CrossRef]
24. Lorenzi, G.; Lanzini, A.; Santarelli, M.; Martin, A. Exergo-economic analysis of a direct biogas upgrading process to synthetic natural gas via integrated high-temperature electrolysis and methanation. *Energy* **2017**, *141*, 1524–1537. [CrossRef]
25. Giglio, E.; Lanzini, A.; Santarelli, M.; Leone, P. Synthetic natural gas via integrated high-temperature electrolysis and methanation: Part II-Economic analysis. *J. Energy Storage* **2015**, *2*, 64–79. [CrossRef]
26. Barrera, R.; Salazar, C.; Pérez, J.F. Thermochemical equilibrium model of synthetic natural gas production from coal gasification using Aspen Plus. *Int. J. Chem. Eng.* **2014**, *2014*, 192057. [CrossRef]
27. Juraík, M.; Sues, A.; Ptasinski, K.J. Exergetic evaluation and improvement of Biomass-to-synthetic natural gas conversion. *Energy Environ. Sci.* **2009**, *2*, 791–801. [CrossRef]
28. Khesa, N.; Mulopo, J. Performance evaluation, Optimization and exergy analysis of a high temperature co-electrolysis power to gas process using Aspen Plus®—A model based study. *Energy Sci. Eng.* **2021**, *9*, 1950–1960. [CrossRef]
29. Juraščík, M.; Sues, A.; Ptasinski, K.J. Exergy analysis of synthetic natural gas production method from biomass. *Energy* **2010**, *35*, 880–888. [CrossRef]
30. Duret, A.; Friedli, C.; Maréchal, F. Process design of Synthetic Natural Gas (SNG) production using wood gasification. *J. Clean. Prod.* **2005**, *13*, 1434–1446. [CrossRef]
31. Al Zakwani, S.; Ouadi, M.; Mohammed, K.; Steinberger-Wilckens, R. Simulation of Biomass Gasification and Syngas Methanation for Methane Production with H_2/CO Ratio Adjustment in Aspen Plus. *Energies* **2025**, *18*, 4319. [CrossRef]